

DISRUPTION LIMITATION TO THE BEAM-BEAM TUNE SHIFT IN CIRCULAR COLLIDERS

S. V. Milton and L. Z. Rivkin

Paul Scherrer Institute, CH-5232, Villigen PSI, Switzerland

ABSTRACT

The beam-beam tune shift parameter, ξ , has been an important input in the initial design of e^+e^- circular colliders. Its use should be questioned in light of two facts. The first is the large, and as yet unexplained, differences in the maximum tune shifts observed in various existing machines (variations from 0.02–0.06). The second is the tendency observed in more recent designs of simultaneously specifying a large ξ and a σ_s/β^* ratio close to or even possibly less than 1. Experimental evidence suggests that a more suitable design parameter is the amplitude disruption parameter defined as $\mathcal{D}^* \equiv ((4\pi\xi)^2 + \mathcal{D}^2)^{1/2}$, where $\mathcal{D} = 4\pi\xi\sigma_s/\beta^*$ is the usual disruption parameter. This observation is further checked with a particle tracking simulation. Designs using a \mathcal{D}^* of 0.6–0.8 seem appropriate.

INTRODUCTION

Machine luminosity (per bunch) has risen substantially since the first colliding beam experiments were performed. Much of this increase can be attributed to decreases in the value of β^* , the beam envelope function at the collision point. However, as β^* continues to decrease its value can become comparable to the bunch length, σ_s . This is particularly true in the vertical direction, i.e. the case of flat beams, which is the focus of this paper. There are indications from theory¹, experiment², and simulation³ which suggest that the ratio $\sigma_s/\beta^* \equiv \zeta$ has a dramatic influence on colliding beam performance. In particular, these authors have found that beam enlargement from the beam-beam interaction (BBI) as a function of current tends to be larger, i.e. a lower peak value of ξ , the larger the ζ . This behavior has been attributed to beam-beam driven synchrotron resonances. As ζ becomes large (i.e. ≥ 1) ξ may no longer be a good design parameter. A new parameter useful for initial design purposes in this new regime should be sought out.

Definitions

As a particle travels through the oncoming beam it not only receives an angular kick, but also, if it has a non-zero longitudinal displacement, s , from the IP at the time of passage through the opposing bunch, it will receive a net transverse displacement as viewed at the IP (fig. 1).

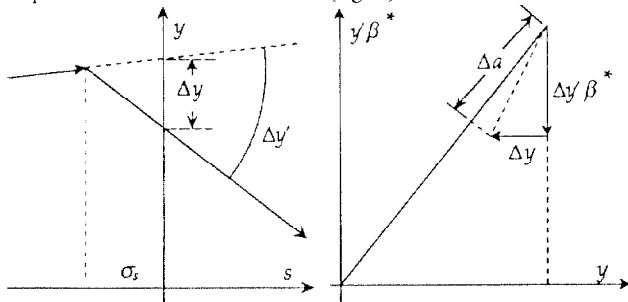


Figure 1: Two views of the instantaneous beam-beam kick.

Consider only the vertical direction and assume for the moment that the BB kick is instantaneous and is applied as the particle passes the longitudinal center of the opposing bunch. In the linear regime, the BBI changes the particle's angle by $\Delta y'/y' = -\beta_y^* f_y = -4\pi\xi_y$, where β_y^* is the vertical beta function at the IP, ξ_y is the vertical tuneshift parameter, and f_y is the vertical focal length of the beam-beam lens given by

$$\frac{1}{f_y} = \frac{2Nr_e}{\gamma\sigma_y(\sigma_x + \sigma_y)}$$

N is the number of particles in the opposing bunch, r_e is the classical radius of the electron, γ is the relativistic factor of the

particle, and σ_x and σ_y are the transverse bunch sizes of the opposing beam at the IP (horizontal and vertical respectively). The change in the particle's displacement (also viewed at the IP) is $\Delta y/y = -s/f_y = -4\pi\xi_y\sigma_s/\beta_y^*$. Here we have assumed the particle to have an average longitudinal displacement σ_s . (Note: Beta varies quadratically from the IP. In the above approximation, this will reduce both $\Delta y'/y'$ and $\Delta y/y$ by $\approx 1/(1 + (\sigma_s/\beta_y^*)^2)^{1/2}$. Since this is the same for both ratios it has been ignored.) The term $4\pi\xi$ will be referred to as the angular disruption, although elsewhere the angular disruption has been defined in a slightly different way⁴. $\mathcal{D} \equiv \Delta z/z = 4\pi\xi\sigma_s/\beta^*$ has been called the disruption⁵; we will continue with this usage. (z is used generically for either transverse direction.)

Another disruption parameter can be constructed. This will be called the amplitude disruption parameter and will be defined as

$$\mathcal{D}^* \equiv \sqrt{(\Delta z/z)^2 + (\Delta z'/z')^2} = \sqrt{\mathcal{D}^2 + (4\pi\xi)^2}$$

\mathcal{D}^* is representative of the average change in a particle's fractional amplitude, $\Delta a/a$, as it passes through the opposing bunch (fig. 1). In the limit of $\zeta \rightarrow 0$, $\mathcal{D}^* \sim 4\pi\xi$, and in the limit $\zeta \gg 1$, $\mathcal{D}^* \sim \mathcal{D}$. Anticipating the results, if \mathcal{D}^* is a constant at peak colliding beam performance (i.e. independent of ζ), $4\pi\xi$ and \mathcal{D} would behave as shown in Fig. 2.

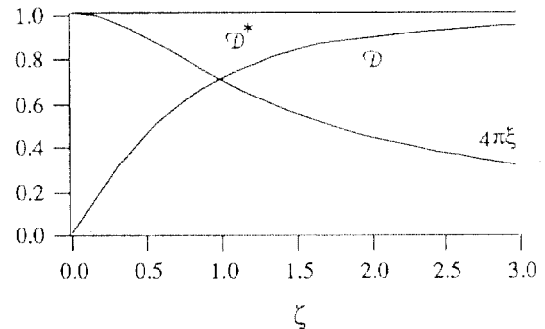


Figure 2: The behavior of \mathcal{D} and $4\pi\xi$ for a constant \mathcal{D}^* .

References 1–3 have already shown the importance of ζ on the resulting colliding beam performance. The question now remains: is there evidence proving that any one of these 3 disruption quantities is a constant in storage rings independent of ζ and, therefore, a useful design tool?

EXISTING EXPERIMENTAL EVIDENCE

CESR Data

A 3 day machine study was performed at the Cornell e^+e^- storage ring CESR in an attempt to determine the β_y^* value which would allow CESR to achieve peak luminosity². Four different values were tried: 5.0 cm, 3.0 cm, 2.0 cm, and 1.5 cm. The horizontal β_x^* was not varied, nor was the bunch length which remained constant at 2.2 cm. Also, since CESR typically runs with nonzero horizontal dispersion at the IP of approximately 0.7 m, all four test lattices were designed with horizontal η^* within the range 0.65–0.70 m. With each lattice an attempt was made to optimize the machine luminosity over a period of 10–20 hours. Optimization was based on the peak luminosity obtained without exceeding beam lifetime or detector background limitations.

Results from this study showing the maximum achieved values of the 3 disruption parameters are shown in Fig. 3. Peak usable luminosity at the $\zeta = 1.5$ point was limited by excessively large singles rates into one of the two experimental detectors rather than being limited by beam lifetime as were the other lattices. The reason for this, given in ref. 2, was that β_y

became very large due to the small β^* , thus creating a vertical aperture limit near the IP. This difference in criteria may be a possible explanation for the slightly lower \mathcal{D}^* value @ $\zeta = 1.5$.

It is difficult to draw definite conclusions from such a limited set of data; however, comparison with Fig. 2 suggest that \mathcal{D}^* is the most likely candidate for being a limiting constant representative of colliding flat-beam performance.

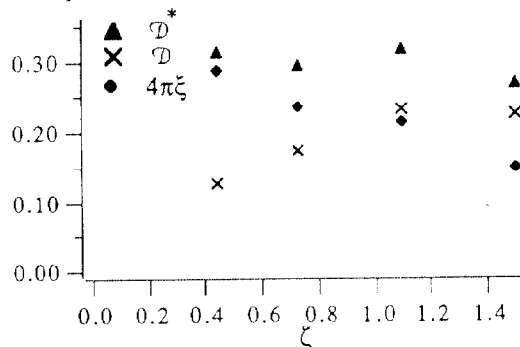


Figure 3: Results from the CESR machine study.

Results From Other Machines

A compilation has also been made of peak machine performance in various machines⁶. These results are shown in table 1 and are plotted in Fig. 4. Comparison of the data is complicated for a number of reasons. For example, operating conditions at each machine are different, and each machine throughout its colliding beam history has experienced its own peculiar set of difficulties limiting its performance in one way or another. These have not been taken into account, nor have other effects such as the influence of the machine tune and perturbation of β^* by the beam-beam lens.

Table 1

Machine	ζ	$4\pi\xi$	\mathcal{D}	\mathcal{D}^*
CESR	1.13	0.25	0.28	0.38
SPEAR	0.45	0.63	0.28	0.69
PEP	0.39	0.63	0.25	0.67
VEPP-4	0.32	0.75	0.24	0.79
VEPP-2M (off)	0.40	0.63	0.25	0.68
VEPP-2M (on)	0.625	0.56	0.35	0.67
PETRA	0.17	0.30	0.051	0.31
DORIS II	0.20	0.31	0.063	0.32
ACO	0.075	0.38	0.028	0.38
DCI	0.035	0.52	0.018	0.52

(on) Wiggler on; (off) Wiggler off

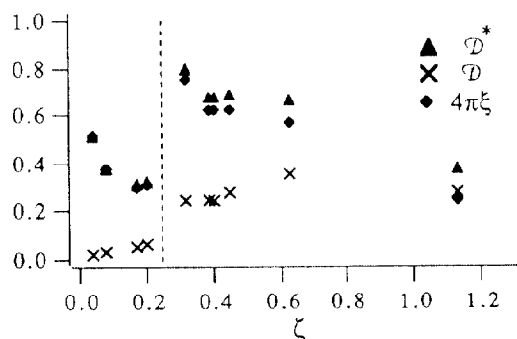


Figure 4: Results from various machines.

These differences aside, one can make the following observations: 1) The results seem to be separated into two groups defined by the line at $\zeta = 0.25$. The cause of this separation is not known, nor will any speculation be put forth. It should be noted however that both the ACO and DCI machines, both of which fall on the low ζ side of the line, were

operated on the coupling resonance with approximately round beams and thus may not compare well with the other flat beam machines. 2) Within each group there is a tendency for $4\pi\xi$ and \mathcal{D}^* to decrease and \mathcal{D} to increase as ζ increases. Most of the variation in \mathcal{D}^* is seen to be due to the variation of $4\pi\xi$. 3) \mathcal{D} appears to saturate at a level of ≈ 0.3 as ζ becomes large. 4) Two extra notes about the CESR data should be made. CESR is the only machine to purposely operate with a very large non-zero dispersion. This fact may make the CESR data "special" compared to other flat beam machines. Also, the values shown for CESR in Fig. 4 are higher than the equivalent points in Fig. 3. This is because Fig. 4 represents the "best" CESR performance and not just the optimum after tuning for a short period of time as in a machine study.

Again it is difficult to draw conclusions from the limited data. As was seen in the previous studies (ref.1-3), the data does confirm that the 3 quantities are dependent in some way on ζ .

PRELIMINARY EXPLORATIONS BY SIMULATION

Description

A simulation of the beam-beam effect in storage rings was used to further explore how variations of ζ affect colliding beam performance. The code used draws much of its structure from the skeleton of one written for strong-strong (S/S) simulation by Jackson⁷, LINØ. Besides being modified to a weak-strong (W/S) version, other modifications and diagnostics have been added as new information on the correct methods of simulating the BBI become available. Most notably, the BB kick has been divided longitudinally into many smaller kicks in order to more closely mimic the actual distributed nature of the particle trajectory through the opposing beam. Also, all beam distributions, synchrotron radiation, damping, and RF are done at a machine symmetry point in order to reduce spurious unphysical correlations.

The transport around one full machine turn has been divided up as follows. Beam initialization is done at the machine symmetry point 1/2 way through the BB kick. The particles are propagated through 1/2 the BB kick. Particles are then transported by linear R matrix 1/2 way around the machine to another machine symmetry point. At this point radiation excitation, damping and RF is applied to the particle coordinates. Transport back to the IP is done using a "mirror symmetric" R matrix (i.e. in 1-dim $R_{11} \longleftrightarrow R_{22}$). Particles are propagated through 1/2 the BB kick. Midway through the BB kick all the bunch characteristics are calculated. This process between the \bullet 's is repeated for many machine turns. No machine errors are considered; however, it has been shown that these have the effect of dramatically increasing the BBI induced beam blowup⁸. Linear lattice coupling has also not been included.

The W/S simulation is made to imitate some S/S characteristics by repeatedly updating the beam sizes used for the BB kick calculation to equal those of the weak beam's. This is done by tracking 512 particles through a fixed strong beam field for a total of $\tau/5T_0$ turns, where τ is the transverse damping time and T_0 is the revolution period. During this time the average RMS sizes of the weak beam is computed. At the end of this period the "strong beam sizes" are updated with the computed weak beam RMS sizes. (This, of course, presupposes gaussian bunches, which is known to not be entirely correct during colliding beam conditions.) The particles are tracked for a total of 3-4 τ . At the end of this period all backup files, histograms, etc. are accumulated and written to disk for latter analysis.

Only symmetric colliders were considered, the reference machine being 5.3 GeV x 5.3 GeV. Typical transverse damping times for these machines are on the order of 10,000 turns. Because of computer limitations, damping rates used in the simulations were 10 times greater, i.e. $\approx 1,000$ turns. Variation

of the damping rates have already been shown by simulation to have an effect on the strength of the BB driven resonances⁹. In particular, the larger the damping rate the less effective a resonance is in enlarging the beam size.

Preliminary Results

Two tune plane locations were explored. One was chosen to be near the normal CESR operating point ($Q_x = 0.72$, $Q_y = 0.675$, $Q_s = 0.03$) in order to allow preliminary comparison to the available experimental data. A second low tune operating point was chosen at the tunes $Q_x = 0.07$, $Q_y = 0.07$, and $Q_s = 0.06$. Its choice was based on the fact that this region of the tune plane is relatively resonance free. The exact choice of the tunes was made by doing a rough tune scan near these regions looking for a minimum in the blowup of the beam thus avoiding major resonances. Only the fractional part of the tunes are considered.

A different optimization criteria than used in the CESR experiment was required with the simulation. In the CESR experiment, lifetimes and backgrounds were used as the criteria for limiting the current and thus the peak luminosity. Computer limitations prohibited determination of the beam lifetimes. The following procedure was used instead. A set of conditions specifying some ζ were chosen. The current was then raised until both $4\pi\xi$ and \mathcal{D} saturated. Plots of the saturated \mathcal{D}^* , \mathcal{D} , and $4\pi\xi$ versus ζ were then made.

Fig. 5 shows the simulation results at the CESR operating point. As in the machine study experiment, ζ was scanned by varying β_y^* while holding $\beta_x^* = 1.1$ m and $\eta_x^* = 0.7$ m. The qualitative similarity of these simulated curves with those of Fig. 2 is very apparent. The resulting curves also look similar to those seen in the experiment (fig. 3); however, the simulation overestimates the values by ≈ 3 -4. A large fraction of this difference is probably due to the different criteria used during optimizing (i.e. saturation vs. particle loss). In the simulation, saturation of $4\pi\xi$ and \mathcal{D} occur at currents of ≈ 2 times higher than those reached in the experiment. The simulation is also inherently prone to achieving higher final values since, in the limit of its own approximations, it is a perfect machine. The same can not be said for the real machine. A third reason for the difference is due to the higher damping rates used in the simulation.

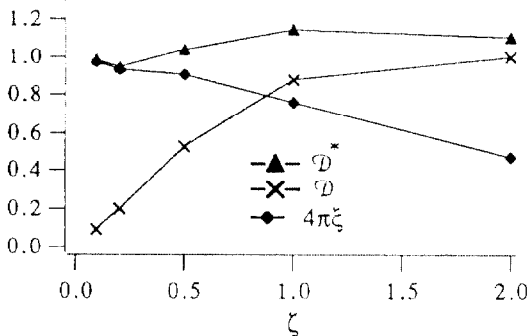


Figure 5: Simulated disruption parameters at the CESR operating point.

Further simulations were done at the second low tune operating point. After an initial run similar to the CESR tune point scan (i.e. vary β_y^* but not β_x^*) which yielded plots similar to Fig. 5, a more controlled set of initial conditions was explored. Fig. 6 shows the results of such a series of runs. In this set of scans the initialized tune shift parameters in each plane were made equal to one another by varying simultaneously β_x^* with β_y^* . This maintains the shape of the beam "footprint" in the tune plane. Dispersion at the IP was set to zero. Saturated values of $4\pi\xi$ and \mathcal{D} were then found. A further, essentially identical, scan was performed, but rather than varying the β 's, σ_s

was varied. The results of this scan was very similar to that of Fig. 6.

The data in Fig. 6 deviates more from Fig. 2 than do the data in Fig. 5. Most notable is the peculiar dip seen at $\zeta \approx 0.7$. This is not understood at this time. It could be due to some complex phenomena (ref. 1 Krishnagopal and Siemann) or something much simpler such as a large population of particles in the tails of the distribution significantly affecting the RMS size calculations. These have not yet been fully checked. However, as a design tool and not a comprehensive theory, the gross characteristics of the curves resemble those of Fig. 2 in which case \mathcal{D}^* is still the favored choice.

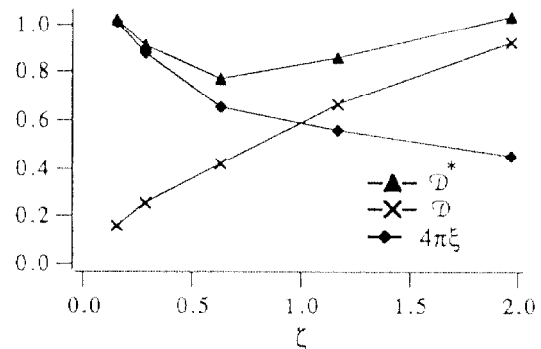


Figure 6: Simulated disruption parameters at the low tune operating point.

SUMMARY

Presently available evidence suggests that \mathcal{D}^* rather than ξ or \mathcal{D} is the proper choice for a parameter useful in designing future machines. The findings do not, however, prove this. Comparison between many different machines is difficult at best and simulation has only been able to give qualitative agreement. The results of the simulation also lead one to believe that the picture is much more complex if one looks closer. Of course more simulations must be done, a more comprehensive theory formed, and many more controlled experiments performed. Until then we believe use of \mathcal{D}^* rather than ξ during the design phase of e^+e^- colliders should be strongly considered. A variation of this has already been applied in a recent design effort¹⁰. A conservative number for \mathcal{D}^* based on past machine performance is in the range 0.6 – 0.8. This is what one may expect of future colliders.

ACKNOWLEDGEMENTS

Yves Baconnier first suggested to us the use of the disruption as a design criterion. We thank him and Werner Joho for many lively discussions regarding this topic.

- 1 S. Krishnagopal and R. H. Siemann, Phys. Rev. D, **41**, 2312 (1990)
- 2 S. Peggs, IEEE Trans on Nucl. Sci., NS-30, No. 4, 2457 (1983).
- 3 D. Rice, CESR Operations Note, CON 87-3 (1987).
- 4 S. Krishnagopal and R. H. Siemann, Cornell Internal Note, CBN 90-2 (1990).
- 5 S. Myers, Nucl. Instr. Methods, **211**, 263 (1983).
- 6 K. Brown, SLAC-PUB-4366.
- 7 R. Hollebeek, Nucl. Inst. Methods, **184**, 333 (1981).
- 8 S. Milton, PSI Preprint, PSI PR-90-05, (1990).
- 9 G. Jackson, Ph.D. Dissertation, Cornell University, (1988).
- 10 A. Piwinski, IEEE Trans. on Nucl. Sci., NS-30, No. 4, 2378 (1983).
- 11 R.H. Siemann, 3rd Adv. ICFA Beam Dynamics Workshop, Novosibirsk, 110 (1989).
- 12 CERN yellow report, CERN 90-02 and PSI PR-90-08, (1990).